



Branched-chain amino acid catabolic defect promotes α -cell proliferation via activating mTOR signaling



Yulin Yang^{a,b,1}, Shushu Wang^{a,b,1}, Chunxiang Sheng^{a,b}, Jialin Tan^{a,b}, Junmin Chen^{a,c}, Tianjiao Li^{a,b}, Xiaoqin Ma^{a,b}, Haipeng Sun^d, Xiao Wang^{a,b,**}, Libin Zhou^{a,b,*}

^a Department of Endocrine and Metabolic Diseases, Shanghai Institute of Endocrine and Metabolic Diseases, Ruijin Hospital, Shanghai Jiao Tong University School of Medicine, Shanghai, China

^b Shanghai National Clinical Research Center for Metabolic Diseases, Key Laboratory for Endocrine and Metabolic Diseases of the National Health Commission of the PR China, Shanghai National Center for Translational Medicine, Ruijin Hospital, Shanghai Jiao Tong University School of Medicine, Shanghai, China

^c Academy of Integrative Medicine, Shanghai University of Traditional Chinese Medicine, Shanghai, China

^d NHC Key Laboratory of Hormones and Development, Tianjin Key Laboratory of Metabolic Diseases, Center for Cardiovascular Diseases, The Province and Ministry Co-sponsored Collaborative Innovation Center for Medical Epigenetics, Chu Hsien-I Memorial Hospital & Tianjin Institute of Endocrinology, Tianjin Medical University, Tianjin, 300134, China

ARTICLE INFO

Keywords:

Branched-chain amino acids
Branched-chain alpha-ketoacid dehydrogenase E1 α subunit
 α -cell
Catabolism
mTOR
Glucose metabolism

ABSTRACT

Elevated circulating level of branched-chain amino acids (BCAAs) is closely related to the development of type 2 diabetes. However, the role of BCAA catabolism in various tissues in maintaining glucose homeostasis remains largely unknown. Pancreatic α -cells have been regarded as amino acid sensors in recent years. Therefore, we generated α -cell specific branched-chain alpha-ketoacid dehydrogenase E1 α subunit (BCKDHA) knockout (BCKDHA- α KO) mice to decipher the effects of BCAA catabolism in α -cells on whole-body energy metabolism. BCKDHA- α KO mice showed normal body weight, body fat, and energy expenditure. Plasma glucagon level and glucose metabolism also remained unchanged in BCKDHA- α KO mice. Whereas, the deletion of BCKDHA led to increased α -cell number due to elevated cell proliferation in neonatal mice. In vitro, only leucine among BCAAs promoted aTC1-6 cell proliferation, which was blocked by the agonist of BCAA catabolism BT2 and the inhibitor of mTOR Rapamycin. Like Rapamycin, BT2 attenuated leucine-stimulated phosphorylation of S6 in aTC1-6 cells. Elevated phosphorylation level of S6 protein in pancreatic α -cells was also observed in BCKDHA- α KO mice. These results suggest that local accumulated leucine due to defective BCAA catabolism promotes α -cell proliferation through mTOR signaling, which is insufficient to affect glucagon secretion and whole-body glucose homeostasis.

1. Introduction

Branched-chain amino acids (BCAAs), including leucine, isoleucine, and valine, are essential amino acids, accounting for about 15–25% of total protein intake (Yamamoto et al., 2017). BCAAs not only provide the substrates for protein synthesis, but also act as signaling molecules to regulate cellular metabolism and growth (Zhang et al., 2017). Accumulating evidence demonstrates that elevated circulating BCAAs are closely related to many metabolic diseases, such as insulin resistance (Wang et al., 2011; Würtz et al., 2013), obesity (Newgard et al., 2009),

type 2 diabetes mellitus (T2DM) (Menni et al., 2013), and cardiovascular disease (Flores-Guerrero et al., 2019). Furthermore, a rise of plasma BCAA levels may predict the development of T2DM (Wang et al., 2011; Floegel et al., 2013). Reducing dietary BCAAs or promoting BCAA catabolism improves glucose metabolism and insulin resistance in rodent models (Fontana et al., 2016; Zhou et al., 2019).

All three BCAAs are initially transaminated by branched-chain amino transferases (BCAT1 and BCAT2) to form branched-chain alpha ketoacids (BCKAs). The BCKAs are then irreversibly decarboxylated by the rate-limiting enzyme branched-chain alpha-ketoacid dehydrogenase (BCKDH) complex, and eventually metabolized to acetyl-CoA or

* Corresponding author. Department of Endocrine and Metabolic Diseases, Shanghai Institute of Endocrine and Metabolic Diseases, Ruijin Hospital, Shanghai Jiao Tong University School of Medicine, Shanghai, China.

** Corresponding author. Department of Endocrine and Metabolic Diseases, Shanghai Institute of Endocrine and Metabolic Diseases, Ruijin Hospital, Shanghai Jiao Tong University School of Medicine, Shanghai, China.

E-mail addresses: wangxiao1976@hotmail.com (X. Wang), libinzhou99@hotmail.com (L. Zhou).

¹ Yulin Yang and Shushu Wang contributed equally to this work.

Abbreviations

BCAAs	branched-chain amino acids
T2DM	type 2 diabetes mellitus
mTOR	mammalian target of rapamycin
BCAT	branched-chain amino transferases
BCKAs	branched-chain alpha ketoacids
BCKDH	branched-chain alpha-ketoacid dehydrogenase
BCKDK	branched-chain alpha-ketoacid dehydrogenase kinase
BCKDHA	branched-chain alpha-ketoacid dehydrogenase E1 α subunit
TCA	tricarboxylic acid
RER	respiratory exchange ratio
CCK-8	Cell Counting Kit-8
EdU	5-Ethynyl-2'-deoxyuridine
qRT-PCR	Quantitative real-time PCR
BAT	brown adipose tissue
Gcgr	glucagon receptor

succinyl-CoA for oxidation (Lian et al., 2015). BCKDH is inactivated via phosphorylation by the BCKDH kinase (BCKDK) and activated via dephosphorylation by the mitochondrial phosphatase 2C (PP2Cm, encoded by the gene PPM1K) (Neinast et al., 2019a, b). E1 α subunit of BCKDH (BCKDHA) has been identified as a primary susceptibility gene for both obesity and T2DM (Tiffin et al., 2006). BCKDK expression or activity is increased in the liver and adipose tissue of obese and diabetic rodents, resulting in reduced BCAA oxidation and elevated plasma BCAA levels (Zhou et al., 2019). Conversely, the inhibitor of BCKDK, BT2 promotes BCAA catabolism and decreases their plasma levels, improving glucose tolerance and insulin sensitivity in these animal models (Zhou et al., 2019; White et al., 2018; Blair et al., 2023).

Glucagon secreted from α -cells plays a crucial role in regulating nutrient metabolism and energy homeostasis (Zeigerer et al., 2021). Dysregulation of glucagon is essential for the development of T2DM (Lee et al., 2016). Traditionally, α -cell is believed to be mainly regulated by glucose. However, α -cell has been widely accepted as amino acid sensors in recent years (Dean, 2020). It has been reported that decreased serum amino acids suppress α -cell proliferation and glucagon secretion through mammalian target of rapamycin (mTOR)-dependent signaling (Kim et al., 2017). On the contrary, interrupted glucagon signaling and subsequent hyper-aminoacidemia result in α -cell proliferation and hyperplasia (Dean et al., 2017; Gong et al., 2023). In the pancreas, BCAs appear to be a dominant source of oxidative fuel, accounting for >20% of carbons incorporated into the tricarboxylic acid (TCA) cycle (Neinast et al., 2019a, b). BCAA strongly stimulates hypersecretion of glucagon in diabetic mice (Wada et al., 2021). However, the effect of α -cell BCAA catabolism on its self-physiological function and whole-body energy homeostasis remains elusive.

To elucidate the role of BCAA catabolism in pancreatic α -cell in energy metabolism, we generated mice with α -cell specific deletion of BCKDHA (BCKDHA- α KO). Though BCKDHA- α KO mice displayed normal glucose metabolism and glucagon secretion, BCAA catabolic defect promoted α -cell proliferation via mTOR signaling.

2. Methods

2.1. Experimental animals

The BCKDHA $^{flox/flox}$;Gcg-Cre (BCKDHA- α KO) mice were generated by crossing mice carrying BCKDHA $^{flox/flox}$ allele with mice carrying the iGcg-Cre transgene (purchased from the Jackson Laboratory, #030663). The mBckdha floxed allele were generated by Cyagen (<https://www.cyagen.com/us/en/>) through traditional ES clones selection followed

by blastocyst microinjection. The BCKDHA $^{flox/flox}$ mouse line contains two LoxP sites flanking the exon 4 of the mBckdha gene on Chromosome 7. BCKDHA $^{flox/flox}$ (wild-type [WT]) mice were used as their littermate controls. Genotyping was performed by PCR analysis using specific primers (forward, ATGGCTATGCCATCTCCACACC; reverse, CAAACA-CATCGTTGCCGTCCAC). All mice were maintained on standard rodent chow and subjected to a 12-h light/12-h dark cycle. Male mice were used for all experiments. Animal protocols were approved by the Institutional Animal Care and Use Committee of Shanghai Model Organisms Center, Inc., Shanghai, China (Protocol No. 2020-0045).

2.2. Intraperitoneal glucose, pyruvate, and leucine tolerance test

After fasting for 16 h, 8 weeks adult mice were intraperitoneally injected with D-glucose (1.5 g/kg body weight), pyruvate (2 g/kg body weight), or leucine (0.3 g/kg body weight). Blood glucose concentrations were measured in tail blood by using a portable glucometer (Johnson & Johnson) at baseline, 15, 30, 60, and 120 min after injection.

2.3. Body fat and energy expenditure analysis

To assess fat mass, mice were weighed to obtain total body weight and then placed in the EchoMRI device for measurement. The ratio of fat mass was presented as a percentage of total body weight. Systemic energy metabolism was evaluated by placing male mice in metabolic cages (Columbus Instruments) to measure the respiratory exchange ratio (RER).

2.4. Cell culture

aTC1-6 glucagonoma cells were cultured in DMEM (GIBCO) containing 10% (v/v) fetal bovine serum, 10 mM HEPES, 100 IU/mL penicillin, and 100 mg/ml streptomycin, and incubated in 37 °C, 5% CO₂ incubator. For proliferation assay, aTC1-6 cells were treated with 4 mM leucine (Sigma), 200 μ M BT2 (MCE), and 40 nM Rapamycin (MCE) for 24 h.

2.5. Cell counting kit-8 (CCK-8) assay

For the CCK-8 assay, aTC1-6 cells were seeded in a 96-well plate at a density of 15,000 cells per well. After intervention for 24 h, the cell survival rate was detected by the CCK-8 kit (SB-CCK8, share-bio) according to the manufacturer's protocol. The absorbance at 450 nm was measured using an iMark microplate absorbance reader (Bio-Rad).

2.6. 5-Ethynyl-2'-deoxyuridine (EdU) assay

For the EdU assay, aTC1-6 cells were seeded in a 12-well plate and labeled with 10 μ M EdU for 120 min. Then the cells were washed twice with phosphate-buffered saline (PBS), fixed with 4% paraformaldehyde for 5 min, and rinsed twice with PBS. Cells were briefly permeabilized with 0.3% Triton X-100, rinsed with PBS, and incubated with the Click-iT EdU Alexa Fluor 488 flow cytometry Kit (CellorLab CX002) for 30 min following the manufacturer's protocol. Flow cytometry was performed by using FACS Verse flow cytometers (BD Biosciences, USA) and the data were analyzed using FlowJo Software (FlowJo, LLC, USA).

2.7. Mouse islet isolation

8-week-old male WT and BCKDHA- α KO mice were anesthetized with chloral hydrate (450 mg/kg, Fisher Scientific). The common duct was clamped and cannulated under a dissecting microscope. Pancreatic inflation was accomplished via the bile duct with 2.0–2.5 ml of 0.5 mg/ml collagenase P (Roche, Switzerland). The perfused pancreas was dissected and incubated at 37 °C for 16.5 min. Digestion was terminated by perfusion with 30 mL of cold HBSS + buffer (Hanks' Balanced Salt

Solution with 1% FBS). Digested tissue was sieved through different cell strainer (800 µm, 425 µm and 70 µm in diameter) successively and intact islets were manually handpicked.

2.8. Quantitative real-time PCR (*qRT-PCR*)

Total cell RNA was extracted using TRIzol reagent (Vazyme). Total islet RNA was extracted using a Total RNA Extraction Kit (Promega) according to the manufacturer's protocol. The concentration of total RNA was measured using a NanoDrop ND2000 spectrophotometer from Thermo Scientific. Then, the total RNA was reverse-transcribed using the PrimerScript Reverse Transcript Master Mix (TaKaRa, Japan). Real-time PCR analysis was conducted using QuantStudio Dx Real-Time PCR Instrument (Applied Biosystems). The relative mRNA expression level of each gene was normalized to that of 18 S. The primer sequences used for qRT-PCR were shown in Supplementary Table 1.

2.9. Immunoblot analysis

To extract protein from cells, a cold RIPA lysis buffer was used. The protein concentration was determined using the BCA Protein Assay Kit from Thermo Fisher Scientific. Total cell lysates were separated by polyacrylamide gel electrophoresis and transferred to nitrocellulose membranes. The membranes were probed with primary antibodies against HSP90 (1:1000, Cell Signaling Technology, #4877), p-S6 Ser240/244 (1:1000, Cell Signaling Technology, #9234), S6 (1:1000, Cell Signaling Technology, #9202), or p-BCKDHA (1:1000, Abcam, ab302504). Subsequently, the membranes were incubated with the corresponding horseradish peroxidase-conjugated secondary antibodies. Images were taken by a LAS-4000 Super CCD Remote Control Science Imaging System (Fuji, Tokyo, Japan).

2.10. Immunohistochemistry

Pancreatic tissues were fixed using 4% (v/v) neutral-buffered formalin and embedded in paraffin. For immunostaining analysis, entire pancreatic tissues were continuously sectioned at 5-mm thickness. Firstly, the paraffin sections were dewaxed and hydrated. To block nonspecific binding, the sections were treated with goat serum and then incubated with primary antibodies overnight at 4 °C, followed by incubation with secondary antibodies for 1 h at room temperature. The primary antibodies used were anti-Glucagon (1:500, Abcam, ab10988, mouse), anti-Insulin (1:1000, Dako, A0564, Guinea pig), anti-BCKDHA (1:1000, ABclonal, A21588, rabbit), anti-pS6 (Ser240/244) (1:200, Cell Signaling Technology, 5364, rabbit), and anti-Ki67 (1:200, Abcam, ab15580, rabbit).

For cell quantification, three to four sections covering the entire pancreas per mouse were used. For each quantification category, at least 3 mice per genotype were analyzed. These sections were imaged using a Zeiss LSM 710 confocal microscope. Cell number was manually counted in the islet microscopy images to identify Ki67, p-S6, and glucagon positive cells. A minimum of 1000 α-cells was counted for each experiment. Islet α-cell proliferation (Ki67+ α-cell %) was determined by calculating the percentage of total glucagon/Ki67 double-positive cells out of the total glucagon+ cells. To assess the activation of mTOR signaling, the percentage of p-S6/glucagon double-positive α-cells in glucagon positive α-cells was analyzed. To quantify cell size, images were captured at 20 × magnification and ImageJ (National Institutes of Health) was used to determine the area of each cell.

2.11. Glucagon secretion assay

Fasting plasma glucagon levels were measured in WT and BCKDHA-αKO mice after 16 h of food deprivation. Whole blood samples were drawn into tubes containing Aprotinin (500 KIU/ml of whole blood, Sigma, #A1153). Blood was centrifuged (4 °C, 3000 rpm, 10min) and

plasma samples were collected. Plasma glucagon concentrations were determined by Glucagon ELISA kit according to manufacturer's protocol (Mercodia, #10-1271-01).

2.12. Statistical analysis

All data were presented as the mean ± SEM. Statistical analyses were performed with unpaired Student *t*-test for two groups or two-way ANOVA followed by Bonferroni's post hoc analysis for multiple groups. *P* < 0.05 was considered statistically significant.

3. Results

3.1. Expressions of BCAA catabolism-related genes in human and mouse pancreases

The first process of BCAA catabolism involves the entry of BCAs into cells through large neutral amino acid transporters SLC3A2, SLC7A5, SLC7A8, SLC43A1, and SLC43A2 (Wei et al., 2020; Chung et al., 2015). Then, BCAT1/2 reversibly converts BCAs into branched-chain keto acids, which subsequently undergo oxidative decarboxylation catalyzed by BCKDH. The end products of BCAA oxidation, acetyl-CoA and succinyl-CoA, enter the TCA cycle (Fig. 1A). A quantitative analysis of the whole-body tissue BCAA oxidation using *in vivo* isotope tracing indicated that the pancreas used BCAA carbons to supply about 20% of the TCA carbons (Neinast et al., 2019a, b). About 10.67% and 4.99% leucine in the pancreas turned into succinate and malate respectively, which far exceeded over those in other tissues (Fig. 1B). To gain further insights into BCAA catabolism in pancreas islets, we re-analyzed single-cell RNA sequencing data in human islets from E-MTAB-5061 datasets (Segerstolpe et al., 2016). Interestingly, genes encoding BCAA transporters and catabolic enzymes, including SLC3A2, SLC7A8, BCAT2, BCKDHA, and HMGCL1, displayed relatively high expressions in human islet α and β-cells (Fig. 1C and D). The pseudo temporal analysis of a mouse islets single-cell RNA sequencing dataset (Qiu et al., 2017) indicated a relatively high expression of BCKDHA in pancreatic α-cells at the late embryonic stage E17.5 and at birth (Fig. 1E). We confirmed the protein expression of BCKDHA in mouse islet α-cells at 2 weeks after birth (Fig. 1F).

3.2. BCAA catabolic defect in islet α-cells does not affect the whole-body glucose homeostasis

Considering the high expression of BCKDHA in early postnatal mouse α-cells, we generated BCKDHA-αKO mice by crossing BCKDHA^{flox/flox} mice with iGcg-Cre mice (Fig. 2A). The BCKDHA mRNA and protein expression levels were significantly reduced in the islet of BCKDHA-αKO mice compared to those of WT mice (Fig. 2B and C), indicating successful deletion of BCKDHA in α-cells. Body weight, body fat, and RER were comparable between WT and BCKDHA-αKO mice (Fig. 2D and F). No differences were observed in random and fasting blood glucose between the two genotype mice (Fig. 2G and H). In addition, there was no significant difference in fasting plasma glucagon between BCKDHA-αKO and WT mice (Fig. 2I). Adult BCKDHA-αKO mice displayed normal glucose tolerance (Fig. 2J). Moreover, intraperitoneal pyruvate and leucine tolerance tests exhibited normal hepatic glucose production in BCKDHA-αKO mice (Fig. 2K and L). Therefore, our result suggests that ablation of BCKDHA in α-cell is not sufficient to cause detectable abnormalities in glucagon secretion and glucose metabolism in mice.

3.3. Impaired BCAA catabolism promotes α-cell proliferation in neonatal mice

It has been well recognized that hyper-aminoacidemia stimulates α-cell proliferation (Kim et al., 2017; Dean et al., 2017; Gong et al., 2023). Decreased BCKDHA expression leads to disrupted BCAA

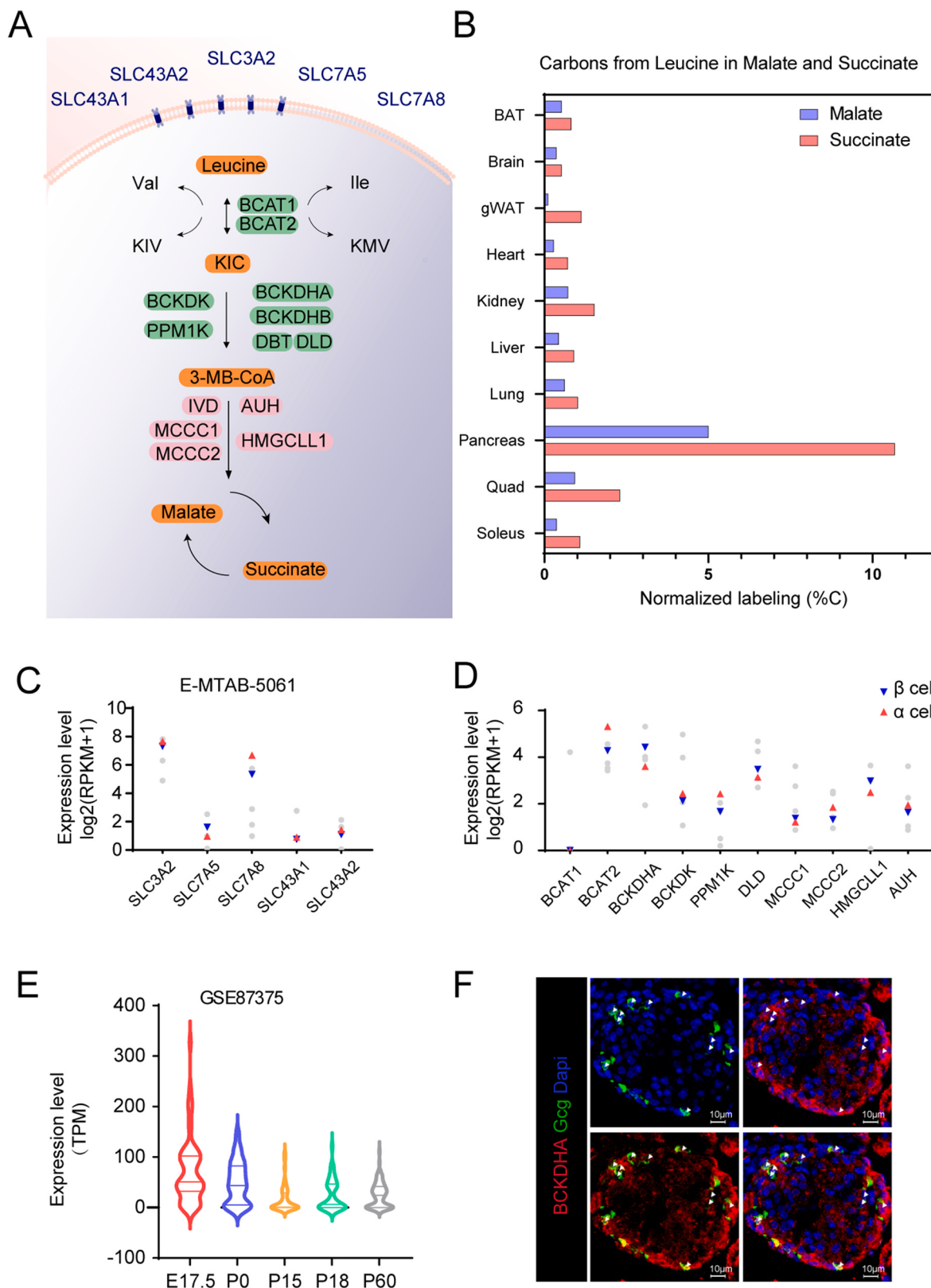
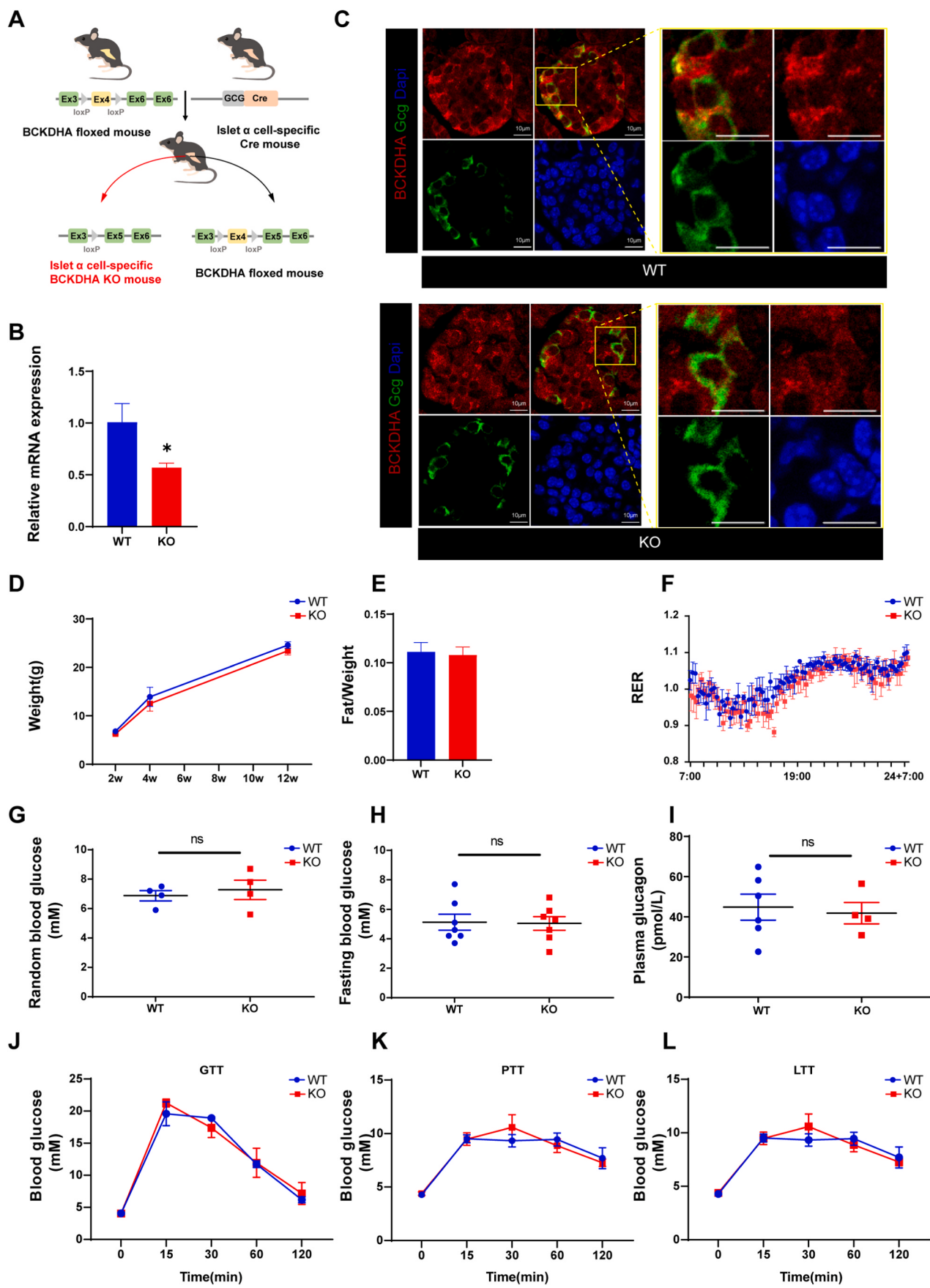


Fig. 1. Expressions of BCAA catabolism-related genes in human and mouse pancreases. (A) Schematic presentation of BCAA uptake and oxidation pathway. (B) Normalized labeling (% carbons normalized) of in vivo leucine isotope tracing (Leucine turned into succinate and malate, respectively). The data are from Cell Metab (2019), 29 (2):417–429. e414. The expression levels of genes encoding (C) BCAA transporters and (D) BCAA catabolic enzymes in human islet α and β -cells from E-MTAB-5061 [\log_2 (RPKM+1)]. (E) Violin plots showing pseudo-temporal analysis of the Bckdha mRNA expression pattern in mouse islet α -cell from GSE87375 (TPM, Transcripts Per Million). (F) Representative pancreatic sections co-immunostained for glucagon (Gcg, green), BCKDHA (red), and Dapi (blue) from 2-weeks WT mice (scale bars, 10 μ m).



(caption on next page)

Fig. 2. Impaired α -cell BCAA catabolism does not affect whole-body energy metabolism. (A) Schematic diagram of generating α -cell specific BCKDHA knockout (BCKDHA- α KO) mice using a Cre-loxP strategy. (B) *Bckdha* mRNA expression in isolated islets from wild-type (WT) and BCKDHA- α KO mice. (C) BCKDHA protein expression in the islets of WT and BCKDHA- α KO mice. Representative pancreatic sections stained with antibodies for glucagon (Gcg, green) and BCKDHA (red) are shown (scale bar, 10 μ m). (D) Body weight ($n = 7$), (E) fat mass ($n = 4$), and (F) Respiratory exchange ratio (RER) ($n = 3$) of adult WT and BCKDHA- α KO mice. (G) Random blood glucose ($n = 4$), (H) Fasting blood glucose ($n = 7$), and (I) Fasting plasma glucagon ($n = 4$ –6) levels of adult 8 weeks WT and BCKDHA- α KO mice. (J) Intraperitoneal glucose tolerance (GTT, $n = 6$ –7), (K) Pyruvate tolerance (PTT, $n = 5$ –6), and (L) Leucine tolerance (LTT, $n = 6$ –7) of WT and BCKDHA- α KO mice. Data are represented as mean \pm SEM. * $P < 0.05$ vs WT.

catabolism and substrate accumulation in macrophages (Zhao et al., 2023), cardiomyocyte (Yu et al., 2023), and brown adipose tissue (BAT) (Yoneshiro et al., 2019). To investigate whether impaired BCAA

catabolism exerts an impact on α -cell proliferation in neonatal period, we analyzed α -cell number at postnatal day 14 when functional α -cell mass had been established (Qiu et al., 2017) and observed an increase in

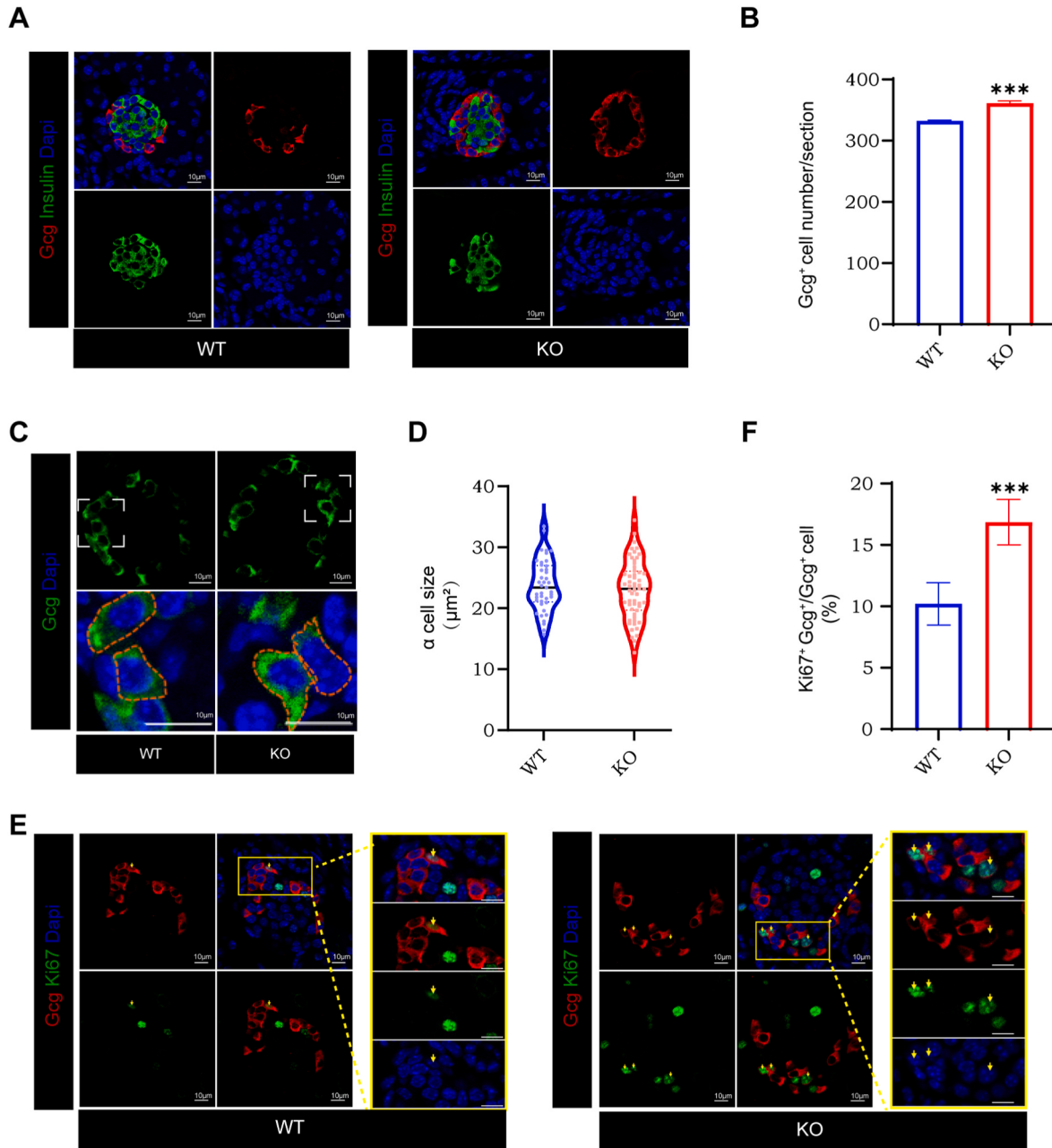


Fig. 3. Disordered α -cell BCAA catabolism promotes α -cell proliferation in BCKDHA- α KO mice. (A) Representative pancreatic sections co-immunostained for glucagon (Gcg, red), insulin (Ins, green), and Dapi (blue) from 2-weeks WT and BCKDHA- α KO mice (scale bars, 10 μ m). (B) Quantification of α -cell number (total glucagon⁺ cells per section) in WT and BCKDHA- α KO mice ($n = 3$). (C) Representative pancreatic sections co-immunostained for glucagon (Gcg, green) and Dapi (blue) in WT and BCKDHA- α KO mice at P7 (scale bars, 10 μ m). (D) The quantitative measurements of α -cell size in Fig. 3C ($n = 3$). (E) Representative pancreatic sections co-immunostained for glucagon (Gcg, red), Ki67 (green), and Dapi (blue) in WT and BCKDHA- α KO mice at P7 (scale bar, 10 μ m). Ki67⁺/glucagon⁺ cells are indicated by yellow arrows. (F) Quantification of α -cells proliferation (percentage of glucagon⁺/Ki67⁺ cells per total glucagon⁺ cells) in WT and BCKDHA- α KO mice at P7 ($n = 3$). Data are represented as mean \pm SEM. *** $P < 0.001$ vs WT group by Student's t-test.

α -cell number in BCKDHA- α KO mice (Fig. 3A and B). But the size of α -cell showed no significant change (Fig. 3C and D). Islet α -cell displayed the highest proliferation rate at postnatal day 7 (P7) as previously reported (Solloway et al., 2015). Therefore, Ki67, a marker of active cell proliferation, and glucagon were costained to assess α -cell proliferation rate in the pancreas tissue sections of WT and BCKDHA- α KO mice at P7. The α -cell proliferation index (percentage of glucagon $^+$ /Ki67 $^+$ cells per total glucagon $^+$ cells) in BCKDHA- α KO mice was markedly increased compared with that in WT mice (Fig. 3E and F). These findings highlight a crucial role of BCAAs in physiological α -cell proliferation during the neonatal period.

3.4. Leucine stimulates α -cell proliferation in vitro

It is reasonable to suppose that the accumulated substrate of BCAA catabolism is the stimulus of neonatal α -cell growth in BCKDHA- α KO

mice. Thus, we treated α TC1-6 cells with leucine, isoleucine, or valine to identify which BCAA is the inducer of α -cell proliferation. As shown in Fig. 4A, 4 mM leucine treatment promoted α TC1-6 cell proliferation in CCK-8 assay, while other two BCAAs were without effect. EdU cell proliferation assay detected a similar result of cell proliferation for leucine (Fig. 4B and C). Cell cycle analysis by flow cytometry revealed that leucine led to an increase in the proportion of α -cells in the S phase (from 28.5% to 32.3%) and S + G2 phase (from 38.3 % to 43.9%) (Fig. 4D and E). BT2, an antagonist of BCKDK, has been widely used to activate BCAA catabolism (Zhou et al., 2019; White et al., 2018; Blair et al., 2023). BT2 blocked leucine-induced BCKDHA phosphorylation at serine 293 (Fig. 4F). BT2 treatment suppressed basal and leucine-induced α TC1-6 cell proliferation as shown in Fig. 4G, H and I by EdU incorporation assay and CCK-8 assay. These results suggest that accumulated leucine stimulates α -cell proliferation when BCAA catabolism is blocked.

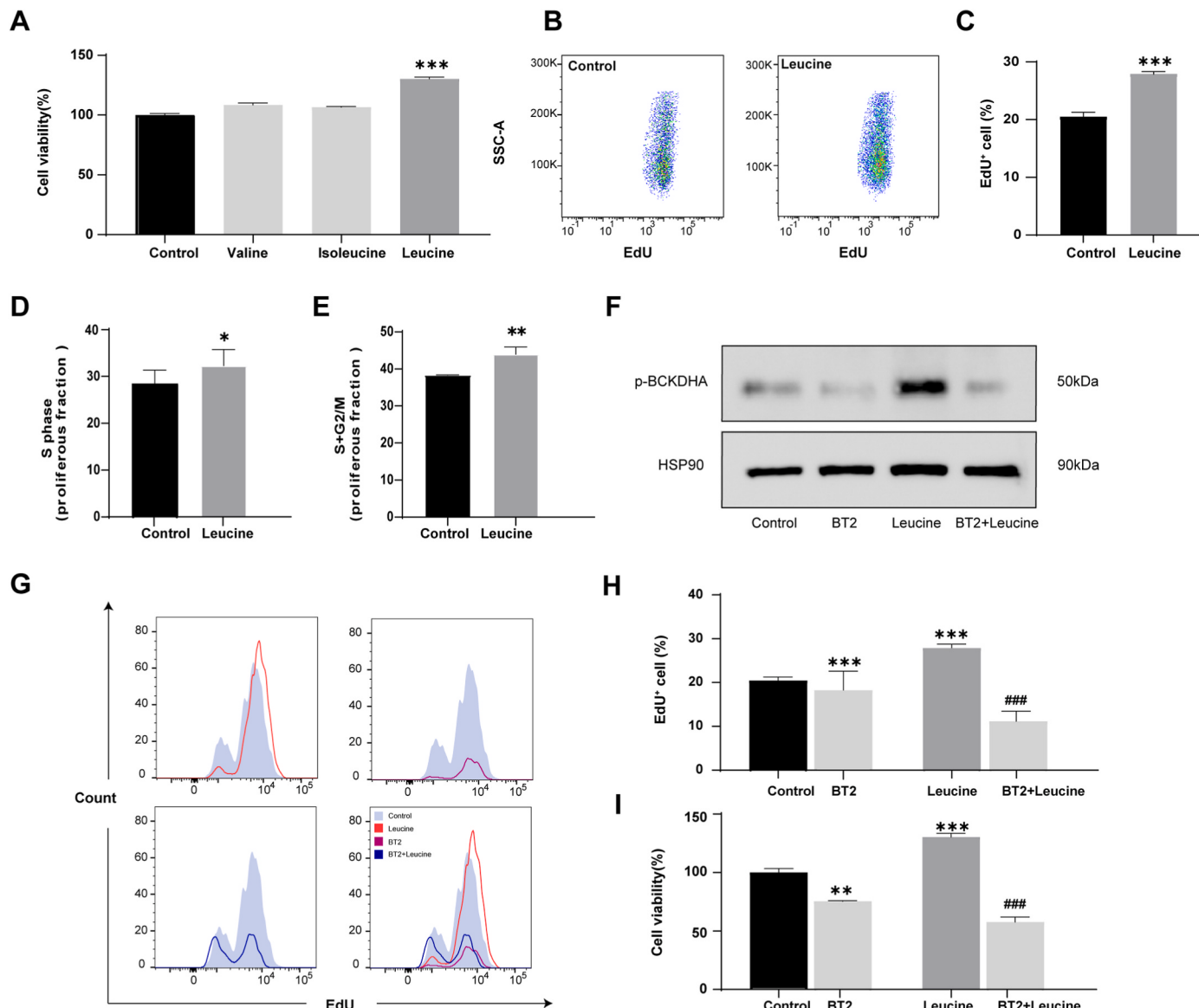


Fig. 4. Leucine increases α -cell proliferation in α TC1-6 cells. (A) Relative growth of α TC1-6 cells incubated with 4 mM of the indicated amino acids for 24 h using CCK-8 analysis ($n = 5$). (B) The proliferation of α TC1-6 cells incubated with 4 mM leucine for 24 h was assessed by EdU staining and flow cytometry analysis. (C) The quantitative measurements of EdU positive rates in Fig. 4B ($n = 3$). (D) Quantification of percentage of cells in S cycle phase ($n = 3$). (E) Quantification of percentage of cells in G2/M cycle phase ($n = 3$). (F) Phosphorylation level of BCKDHA in α TC1 cells treated with 4 mM leucine and 200 μ M BT2 for 2 h. (G) α TC1-6 cells were treated with 4 mM leucine or 200 μ M BT2 for 24 h. Cell proliferation were assessed by EdU staining and flow cytometry analysis. (H) The quantitative measurements of EdU positive rates in Fig. 4G ($n = 3$). (I) Relative growth of α TC1-6 cells treated with 4 mM leucine and 200 μ M BT2 for 24 h using CCK-8 analysis ($n = 5$). Data are represented as mean \pm SEM. ** $P < 0.01$, *** $P < 0.001$ vs control; ### $P < 0.001$ vs leucine alone.

3.5. mTOR activity is responsible for leucine-induced α-cell proliferation

Cells and tissues respond to systemic fluctuations in nutrient availability, and intracellular BCAAs can influence cell proliferation through mTOR signaling (Erickson et al., 2019; Li et al., 2020). To explore the mechanism underlying leucine-induced α-cell proliferation, αTC1-6 cells were treated with leucine and the mTOR inhibitor Rapamycin. Expectedly, Rapamycin significantly inhibited leucine-stimulated αTC1-6 cell proliferation assessed by CCK-8 assay (Fig. 5A). A similar result was observed by EdU incorporation assay (Fig. 5B and C). The expressions of cell cycle stage signature genes (G1/S and G2/M) were further detected. Leucine treatment stimulated the mRNA expressions of G1/S cell-cycle

genes Mcm3 and Cdk2, which were abolished by Rapamycin (Fig. 5D). Rapamycin also antagonized leucine-elicited expressions of G2/M cell-cycle genes Ccnb1 and Cyclin A2 (Fig. 5E). Furthermore, leucine administration promoted S6 phosphorylation in αTC1-6 cells, which was markedly blocked by Rapamycin (Fig. 5F). Consistently, BT2 attenuated leucine-induced S6 phosphorylation level (Fig. 5G).

3.6. Activation of mTOR signaling in α-cell of neonatal BCKDHA-αKO mice

We further detected the change of mTOR signaling in pancreatic α-cells of neonatal BCKDHA-αKO mice. As shown in Fig. 6A and B, the

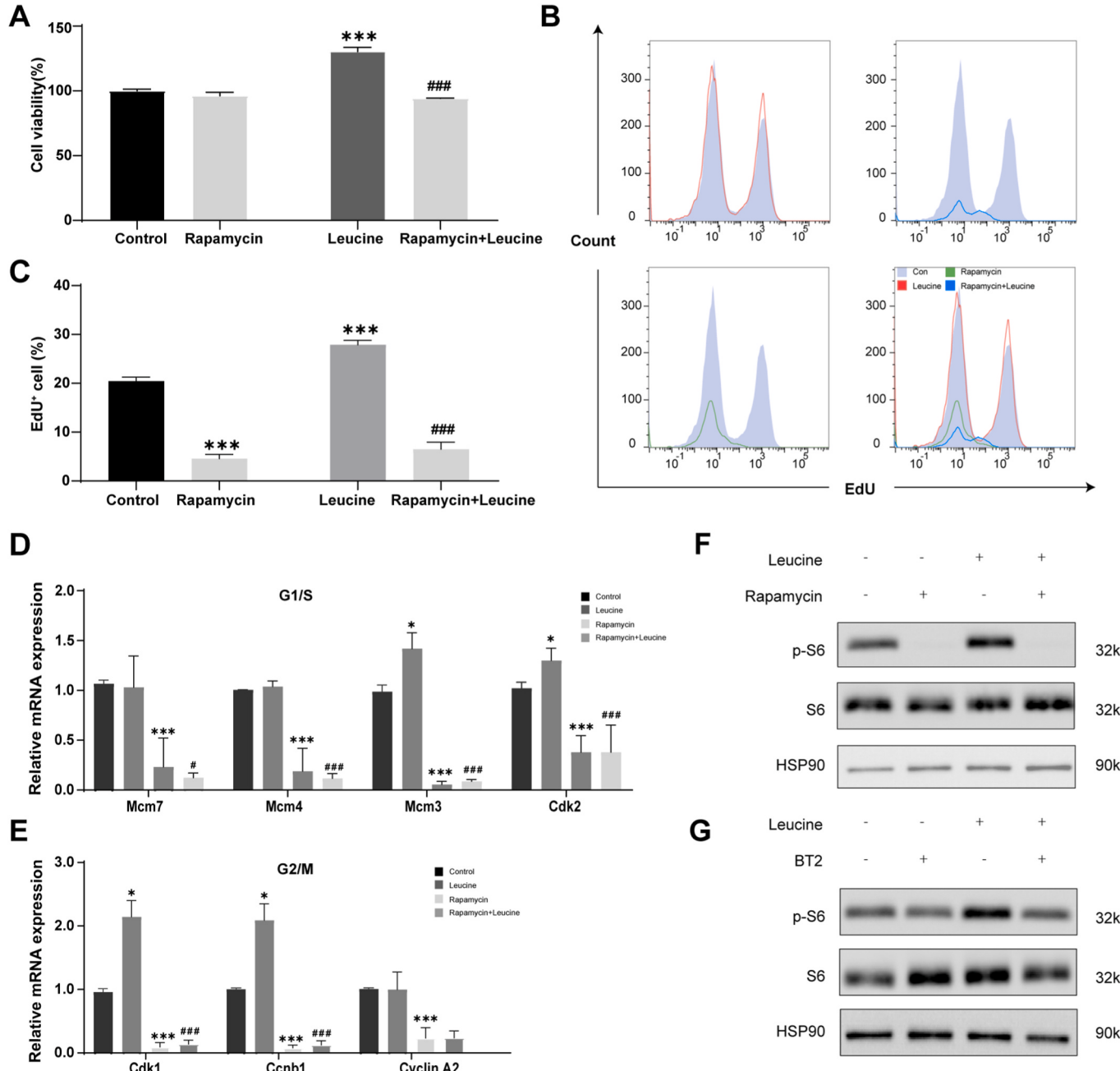


Fig. 5. Leucine stimulates α-cell proliferation by activating mTOR signaling. The proliferation of αTC1-6 cells incubated with 4 mM leucine or 40 nM Rapamycin for 24 h was assessed by (A) CCK-8 analysis ($n = 5$) and (B) EdU staining and flow cytometry analysis. (C) The EdU positive rate is calculated based on Fig. 5B ($n = 3$). mRNA levels of cell cycle (D) G1/S and (E) G2/M genes in αTC-1 cells treated with 4 mM leucine and 40 nM rapamycin for 24 h. (F and G) Phosphorylation level of S6 in αTC-1 cells treated with 4 mM leucine, 40 nM Rapamycin, and 200 μM BT2 for 2 h. Data are represented as mean ± SEM. * $P < 0.05$, ** $P < 0.01$, *** $P < 0.001$ vs control; # $P < 0.05$, ## $P < 0.001$ vs leucine alone.

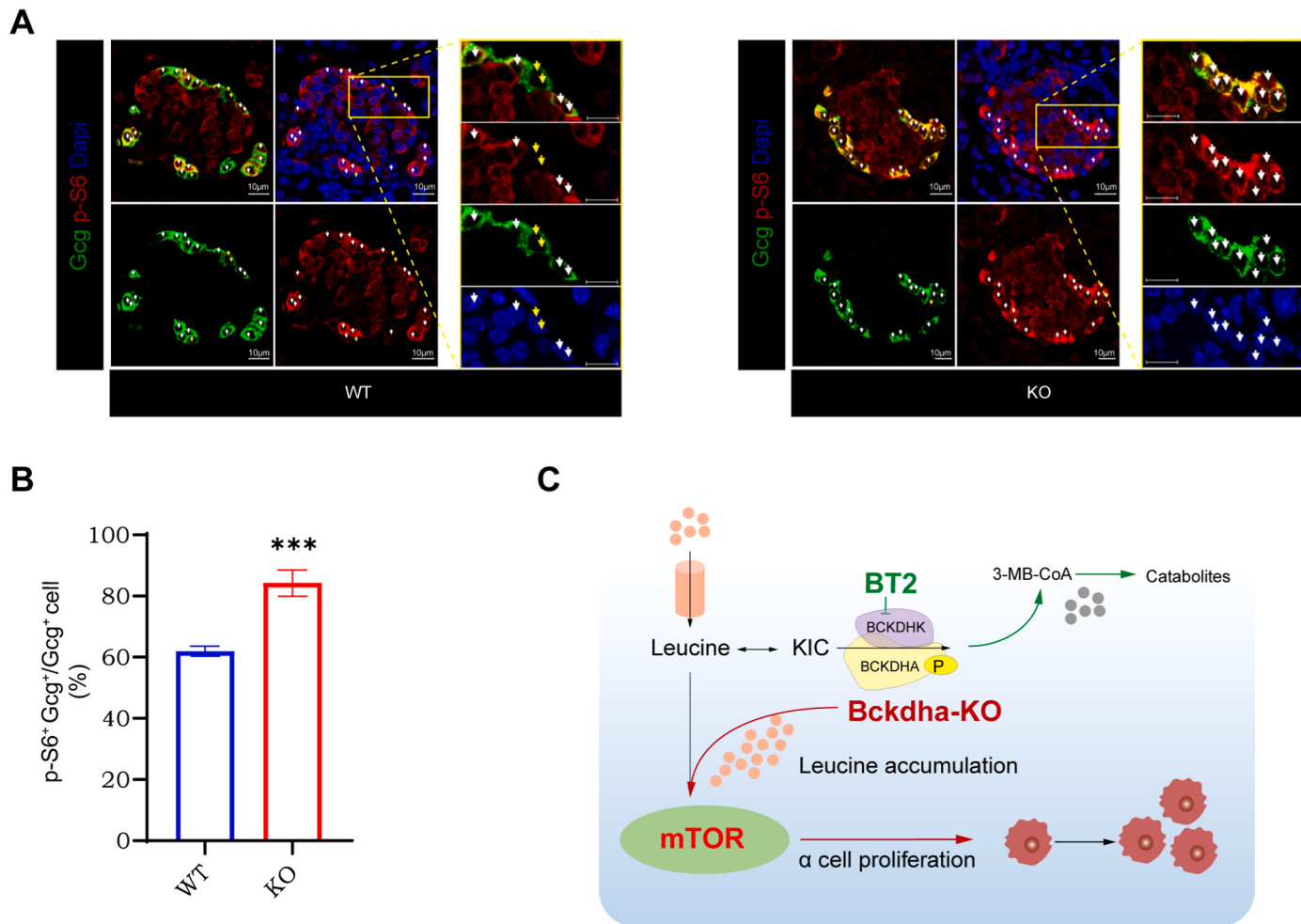


Fig. 6. mTOR signaling activation in pancreatic α -cell of BCKDHA- α KO mice. (A) Representative pancreatic sections co-immunostained for glucagon (Gcg, green), p-S6 (red), and Dapi (blue) from WT and BCKDHA- α KO mice at P7 (scale bars, 10 μ m). p-S6⁺/glucagon⁺ cells are indicated by white arrows, and p-S6/glcagon⁺ cells are indicated by yellow arrows. (B) Quantification of p-S6⁺ cells in glucagon⁺ cells in WT and BCKDHA- α KO mice at P7 ($n = 3$). Data are represented as mean \pm SEM. ***P < 0.001 vs WT. (C) The schematic illustration summarizes the key role of leucine catabolism in α -cell proliferation. Leucine enters into α -cells through amino acid transporters, stimulates mTOR signaling, and promotes α -cell proliferation. When BCKDHA is ablated and leucine catabolism is blocked, local accumulated leucine stimulates α -cell proliferation. On the contrary, BT2 promotes leucine catabolism and inhibits α -cell proliferation via attenuating mTOR signaling.

number of p-S6⁺ cells was significantly increased in α -cells of BCKDHA- α KO mice compared with that in wild-type mice, indicating the activation of mTOR signaling.

4. Discussion

BCAA catabolism has recently been implicated in the development of metabolic diseases. Tissue-specific animal models provide insights into the contribution of BCAA catabolism in various tissues to the whole-body energy homeostasis (Blair et al., 2023; Yoneshiro et al., 2019). In the present study, the deletion of BCKDHA in islet α -cells had no impacts on body weight, body fat, and glucose metabolism in mice. However, BCKDHA- α KO mice exhibited a significant increase in α -cell number due to its proliferation, without change in blood glucagon level. Among BCAs, only leucine stimulated α TC1-6 cell proliferation, which was blocked by BT2, a BCKDK inhibitor. Like Rapamycin, BT2 antagonized leucine-stimulated mTOR signal as well as cell-cycle gene expressions. These results indicate that leucine accumulation due to impaired BCAA catabolism promotes islet α -cell proliferation through mTOR signal pathway (Fig. 6C).

A growing number of studies have linked BCAA metabolism to glucose homeostasis. Elevated circulating levels of BCAs and related metabolites predict the development of T2DM in various study cohorts

(Wang et al., 2011; Long et al., 2020; Arany and Neinast, 2018). Increasing whole-body BCAA oxidation by activating BCKDHA with the BCKDK inhibitor BT2 improves glucose tolerance and insulin sensitivity in obese or diabetic rodents (Zhou et al., 2019; White et al., 2018; Blair et al., 2023). Another BCKDK inhibitor sodium phenylbutyrate also increases insulin sensitivity in type 2 diabetic patients (Vanweert et al., 2022). However, the mechanism underlying the contribution of BCAA catabolism to glucose homeostasis remains unclear. Though skeletal muscle is regarded as the largest contributor of BCAA oxidation, followed by the liver (Neinast et al., 2019a,b), integrated genomic analyses in both human and mouse populations revealed a strong association between glycaemic traits and BCAA catabolic gene expressions in adipose tissue, not in the skeletal muscle (Zhou et al., 2019). In obese or diabetic rodents, BCAT2 and BCKDHA expressions are decreased while BCKDK expression is increased in the liver and adipose tissue (Neinast et al., 2019a, b; She et al., 2007; Lackey et al., 2013). Blocking BCAA catabolism in white adipose tissue by ablation of BCKDHA expression attenuates high fat diet-induced obesity and improves glucose tolerance (Shao et al., 2022). BAT-specific knockout of BCKDHA leads to systemic glucose intolerance and insulin resistance due to impaired BCAA clearance (Yoneshiro et al., 2019). Overexpression of PPM1K in the liver improves glucose tolerance independent of body-weight loss in rats (White et al., 2018). However, the muscle, liver-specific, or combined

tissue deletion of BCKDK had no significant effect on glucose tolerance in mice, despite obvious decreases in plasma BCAA level (Blair et al., 2023). In another study, liver-specific knockout of BCKDHA improves glucose tolerance in mice fed with high fat diet, not in mice fed with chow diet (Nishi et al., 2023). Apparently, it is likely that BCAA catabolism in various tissues plays a distinct role in whole-body energy homeostasis through other signal molecules. BCAA deprivation has been demonstrated to reduce insulin secretion in rats (Horiuchi et al., 2017) while leucine exerts an insulinotropic effect (Neinast et al., 2019a, b). In addition, BCAs increased plasma glucagon levels in diabetic mice and BT2 abolished BCAA-elicited hypersecretion of glucagon in diabetic islets (Wada et al., 2021). However, whether BCAA catabolic defect in pancreatic α -cells is linked to hyperglucagonemia in vivo remains unknown. In the present study, α -cell specific deletion of BCKDHA had no impact on plasma glucagon level and glucose tolerance in mice. Hepatic glucose production was also unchanged in BCKDHA- α KO mice. These results suggest that pancreatic α -cell catabolism of BCAs is insufficient to affect systemic energy metabolism.

Glucagon may be a potential link between animal protein intake and the development of T2DM (Adeva-Andany et al., 2019). Pancreatic α -cell hyperplasia and elevated α -cell proliferation have been observed in multiple mouse models with interrupted glucagon signaling, such as mice treated with glucagon-neutralization antibody (Winther-Sørensen et al., 2020), mice with global glucagon receptor (Gcgr) knockout (Galsgaard et al., 2018), mice with liver-specific deletion of either Gcgr or CaSR (Gong et al., 2023). It has been demonstrated that elevated circulating levels of amino acids act as a trophic stimulus of α -cell proliferation in these models (Dean et al., 2017). The exuberant proliferation of islet α -cell is observed in neonatal period accompanied by relatively higher circulating levels of amino acids during lactation (Solloway et al., 2015). However, the role of BCAs in α -cell proliferation remains unknown. Interestingly, BCKDHA- α KO mice displayed a significant increase in α -cell proliferation at P7 in this current study. It has been demonstrated that BCKDHA knockdown in hepatocytes increases intracellular BCAA contents and cell proliferation rates (Eriksen et al., 2019). Thus, it is reasonable to speculate that elevated neonatal α -cell proliferation is attributed to the local accumulation of BCAA due to impaired BCAA catabolism. We identified leucine as the only stimulus of α Tc1-6 cell proliferation among BCAs. On the contrary, BT2 block leucine-induced α Tc1-6 cell proliferation.

mTOR is a conserved serine/threonine protein kinase that regulates cellular proliferation, growth, motility, and survival (Mossmann et al., 2018). mTOR integrates signals from both growth factors and nutrient abundance (Sancak et al., 2008). Studies have shown that mTOR activity is regulated by BCAA availability (Lynch, 2001), especially elevated extracellular leucine (She et al., 2007). On the other hand, leucine deprivation decreases mTOR activity in liver (Wei, et al., 2018). Decreased serum amino acids were reported to suppress α -cell proliferation by attenuating mTOR signaling (Solloway et al., 2015). Our data demonstrated that leucine specifically promoted α -cell proliferation in a mTOR-dependent manner. Moreover, BT2 blocked leucine-elicited activation of mTOR in α Tc1-6 cell, indicating that promoting leucine catabolism inhibits mTOR signaling in pancreatic α -cells. In recent years, intracellular leucine sensors, including Sar1b (Chen et al., 2021) and Sestrin2 (Sancak et al., 2008) in various tissues have been widely explored. Sar1b, Sestrin2, and other genes related to the nutrient-sensing arm of mTORC1 were expressed in mouse α -cells at different developmental periods based on islet single-cell transcriptomic analysis from GSE87375 (Fig. S1). However, the characteristics and function of leucine sensing in α -cells are generally unknown and need further investigation. Mice with α -cell specific deletion of the mTORC1 regulator Raptor exhibited significantly decreased neonatal α -cell proliferation rate (Bozadjieva et al., 2017). In the present study, increased neonatal α -cell mTOR activity is observed in BCKDHA- α KO mice.

In summary, local accumulated leucine caused by defective BCAA catabolism promotes pancreatic α -cell proliferation through mTOR

signaling in mice. But this does not change plasma glucagon level and glucose homeostasis. The contribution of BCAA catabolism in various tissues to whole energy metabolism need further investigation.

CRediT authorship contribution statement

Yulin Yang: Conceptualization, Data curation, Writing – original draft, Writing – review & editing. **Shushu Wang:** Conceptualization, Data curation, Writing – original draft, Writing – review & editing. **Chunxiang Sheng:** Data curation. **Jialin Tan:** Data curation. **Junmin Chen:** Data curation. **Tianjiao Li:** Data curation. **Xiaoqin Ma:** Data curation. **Haipeng Sun:** Methodology. **Xiao Wang:** Conceptualization. **Libin Zhou:** Conceptualization, Writing – original draft, Writing – review & editing.

Declaration of competing interest

All authors confirm that no conflicts of interest relevant to this article exist.

Data availability

No data was used for the research described in the article.

Acknowledgements

This work was funded by the National Natural Science Foundation of China (82270860 and 82370798) and Shanghai Science and Technology Committee (22140902900).

Appendix A. Supplementary data

Supplementary data to this article can be found online at <https://doi.org/10.1016/j.mce.2023.112143>.

References

- Adeva-Andany, M.M., Funcasta-Calderón, R., Fernández-Fernández, C., Castro-Quintela, E., Carneiro-Freire, N., 2019. Metabolic effects of glucagon in humans. *J. Clin. Transl. Endocrinol.* 15, 45–53.
- Arany, Z., Neinast, M., 2018. Branched chain amino acids in metabolic disease. *Curr. Diabates Rep.* 18, 76.
- Blair, M.C., Neinast, M.D., Jang, C., Chu, Q., Jung, J.W., Axsom, J., Bornstein, M.R., Thorsheim, C., Li, K., Hoshino, A., et al., 2023. Branched-chain amino acid catabolism in muscle affects systemic BCAA levels but not insulin resistance. *Nat. Metab.* 5, 589–606.
- Bozadjieva, N., Blandino-Rosano, M., Chase, J., Dai, X.Q., Cummings, K., Gimeno, J., Dean, D., Powers, A.C., Gittes, G.K., Rüegg, M.A., et al., 2017. Loss of mTORC1 signaling alters pancreatic α -cell mass and impairs glucagon secretion. *J. Clin. Invest.* 127, 4379–4393.
- Chen, J., Ou, Y., Luo, R., Wang, J., Wang, D., Guan, J., Li, Y., Xia, P., Chen, P.R., Liu, Y., 2021. SAR1B senses leucine levels to regulate mTORC1 signalling. *Nature* 596, 281–284.
- Chung, J., Bauer, D.E., Ghamari, A., Nizzi, C.P., Deck, K.M., Kingsley, P.D., Yien, Y.Y., Huston, N.C., Chen, C., Schultz, I.J., et al., 2015. The mTORC1/4E-BP pathway coordinates hemoglobin production with L-leucine availability. *Sci. Signal.* 8 (372), ra34, 2015 Apr 14.
- Dean, E.D., 2020. A primary role for α -cells as amino acid sensors. *Diabetes* 69, 542–549.
- Dean, E.D., Li, M., Prasad, N., Wisniewski, S.N., Von Deylen, A., Spaeth, J., Maddison, L., Botros, A., Sedgeman, L.R., Bozadjieva, N., et al., 2017. Interrupted glucagon signaling reveals hepatic α -cell axis and role for l-glutamine in α -cell proliferation. *Cell Metabol.* 25, 1362–1373.e5.
- Eriksen, R.E., Lim, S.L., McDonnell, E., Shuen, W.H., Vadiveloo, M., White, P.J., Ding, Z., Kwok, R., Lee, P., Radda, G.K., Toh, H.C., Hirshey, M.D., Han, et al., 2019. Loss of BCAA catabolism during carcinogenesis enhances mTORC1 activity and promotes tumor development and progression. *Cell Metabol.* 29, 1151–1165.e6.
- Floegel, A., Stefan, N., Yu, Z., Mühlenbruch, K., Drogan, D., Joost, H.G., Fritsche, A., Häring, H.U., Hrabé de Angelis, M., Peters, A., et al., 2013. Identification of serum metabolites associated with risk of type 2 diabetes using a targeted metabolomic approach. *Diabetes* 62, 639–648.
- Flores-Guerrero, J.L., Groothof, D., Connelly, M.A., Otvos, J.D., Bakker, S.J.L., Dullaart, R.P.F., 2019. Concentration of branched-chain amino acids is a strong risk marker for incident hypertension. *Hypertension* 74, 1428–1435.

- Fontana, L., Cummings, N.E., Arriola Apelo, S.I., Neuman, J.C., Kasza, I., Schmidt, B.A., Cava, E., Spelta, F., Tosti, V., Syed, F.A., et al., 2016. Decreased consumption of branched-chain amino acids improves metabolic health. *Cell Rep.* 16, 520–530.
- Galsgaard, K.D., Winther-Sørensen, M., Ørskov, C., Kissow, H., Poulsen, S.S., Vilstrup, H., Prehn, C., Adamski, J., Jepsen, S.L., Hartmann, B., et al., 2018. Disruption of glucagon receptor signaling causes hyperaminoacidemia exposing a possible liver-alpha-cell axis. *Am. J. Physiol. Endocrinol. Metab.* 314, E93–e103.
- Gong, Y., Yang, B., Zhang, D., Zhang, Y., Tang, Z., Yang, L., Coate, K.C., Yin, L., Covington, B.A., Patel, R.S., et al., 2023. Hyperaminoacidemia induces pancreatic α -cell proliferation via synergism between the mTORC1 and CaSR-Gq signaling pathways. *Nat. Commun.* 14, 235.
- Horiuchi, M., Takeda, T., Takanashi, H., Ozaki-Masuzawa, Y., Taguchi, Y., Toyoshima, Y., Otani, L., Kato, H., Sone-Yonezawa, M., Hakuno, F., et al., 2017. Branched-chain amino acid supplementation restores reduced insulinotropic activity of a low-protein diet through the vagus nerve in rats. *Nutr. Metab.* 14, 59.
- Kim, J., Okamoto, H., Huang, Z., Anguiano, G., Chen, S., Liu, Q., Cavino, K., Xin, Y., Na, E., Hamid, R., et al., 2017. Amino acid transporter Slc38a5 controls glucagon receptor inhibition-induced pancreatic α -cell hyperplasia in mice. *Cell Metabol.* 25, 1348–1361.e8.
- Lackey, D.E., Lynch, C.J., Olson, K.C., Mostaed, R., Ali, M., Smith, W.H., Karpe, F., Humphreys, S., Bedinger, D.H., Dunn, T.N., et al., 2013. Regulation of adipose branched-chain amino acid catabolism enzyme expression and cross-adipose amino acid flux in human obesity. *Am. J. Physiol. Endocrinol. Metab.* 304, E1175–E1187.
- Lee, Y.H., Wang, M.Y., Yu, X.X., Unger, R.H., 2016. Glucagon is the key factor in the development of diabetes. *Diabetologia* 59, 1372–1375.
- Li, J.T., Yin, M., Wang, D., Wang, J., Lei, M.Z., Zhang, Y., Liu, Y., Zhang, L., Zou, S.W., Hu, L.P., et al., 2020. BCAT2-mediated BCAA catabolism is critical for development of pancreatic ductal adenocarcinoma. *Nat. Cell Biol.* 22, 167–174.
- Lian, K., Du, C., Liu, Y., Zhu, D., Yan, W., Zhang, H., Hong, Z., Liu, P., Zhang, L., Pei, H., et al., 2015. Impaired adiponectin signaling contributes to disturbed catabolism of branched-chain amino acids in diabetic mice. *Diabetes* 64, 49–59.
- Long, J., Yang, Z., Wang, L., Han, Y., Peng, C., Yan, C., Yan, D., 2020. Metabolite biomarkers of type 2 diabetes mellitus and pre-diabetes: a systematic review and meta-analysis. *BMC Endocr. Disord.* 20, 174.
- Lynch, C.J., 2001. Role of leucine in the regulation of mTOR by amino acids: revelations from structure-activity studies. *J. Nutr.* 131, 861s–865s.
- Menni, C., Fauman, E., Erte, I., Perry, J.R., Kastenmüller, G., Shin, S.Y., Petersen, A.K., Hyde, C., Psatha, M., Ward, K.J., et al., 2013. Biomarkers for type 2 diabetes and impaired fasting glucose using a nontargeted metabolomics approach. *Diabetes* 62, 4270–4276.
- Mossmann, D., Park, S., Hall, M.N., 2018. mTOR signalling and cellular metabolism are mutual determinants in cancer. *Nat. Rev. Cancer* 18, 744–757.
- Neinast, M., Murashige, D., Arany, Z., 2019a. Branched chain amino acids. *Annu. Rev. Physiol.* 81, 139–164.
- Neinast, M.D., Jang, C., Hui, S., Murashige, D.S., Chu, Q., Morscher, R.J., Li, X., Zhan, L., White, E., Anthony, T.G., et al., 2019b. Quantitative analysis of the whole-body metabolic fate of branched-chain amino acids. *Cell Metabol.* 29, 417–429.e4.
- Newgard, C.B., An, J., Bain, J.R., Muehlbauer, M.J., Stevens, R.D., Lien, L.F., Haqq, A.M., Shah, S.H., Arlotto, M., Slentz, C.A., et al., 2009. A branched-chain amino acid-related metabolic signature that differentiates obese and lean humans and contributes to insulin resistance. *Cell Metabol.* 9, 311–326.
- Nishi, K., Yoshii, A., Abell, L., Zhou, B., Frausto, R., Ritterhoff, J., McMillen, T.S., Sweet, I., Wang, Y., Gao, C., et al., 2023. Branched-chain keto acids inhibit mitochondrial pyruvate carrier and suppress gluconeogenesis in hepatocytes. *Cell Rep.* 42, 112641.
- Qiu, W.L., Zhang, Y.W., Feng, Y., Li, L.C., Yang, L., Xu, C.R., 2017. Deciphering pancreatic islet β cell and α -cell maturation pathways and characteristic features at the single-cell level. *Cell Metabol.* 25, 1194–1205.e4.
- Sancak, Y., Peterson, T.R., Shaul, Y.D., Lindquist, R.A., Thoreen, C.C., Bar-Peled, L., Sabatini, D.M., 2008. The Rag GTPases bind raptor and mediate amino acid signaling to mTORC1. *Science* 320, 1496–1501.
- Segerstolpe, Å., Palasantza, A., Eliasson, P., Andersson, E.M., Andréasson, A.C., Sun, X., Picelli, S., Sabirish, A., Clausen, M., Bjursell, M.K., et al., 2016. Single-cell transcriptome profiling of human pancreatic islets in health and type 2 diabetes. *Cell Metabol.* 24, 593–607.
- Shao, J., Liu, Y., Zhang, X., Shu, L., Yu, J., Yang, S., Gao, C., Wang, C., Cao, N., Zhou, M., et al., 2022. BCAA catabolism drives adipogenesis via an intermediate metabolite and promotes subcutaneous adipose tissue expansion during obesity. *bioRxiv* 2022, 08.18.504380.
- She, P., Van Horn, C., Reid, T., Hutson, S.M., Cooney, R.N., Lynch, C.J., 2007. Obesity-related elevations in plasma leucine are associated with alterations in enzymes involved in branched-chain amino acid metabolism. *Am. J. Physiol. Endocrinol. Metab.* 293, E1552–E1563.
- Solloway, M.J., Madjidi, A., Gu, C., Eastham-Anderson, J., Clarke, H.J., Kljavin, N., Zavala-Solorio, J., Kates, L., Friedman, B., Brauer, M., et al., 2015. Glucagon couples hepatic amino acid catabolism to mTOR-dependent regulation of α -cell mass. *Cell Rep.* 12, 495–510.
- Tiffin, N., Adie, E., Turner, F., Brunner, H.G., van Driel, M.A., Oti, M., Lopez-Bigas, N., Ouzounis, C., Perez-Iratxeta, C., Andrade-Navarro, M.A., et al., 2006. Computational disease gene identification: a concert of methods prioritizes type 2 diabetes and obesity candidate genes. *Nucleic Acids Res.* 34, 3067–3081.
- Vanweert, F., Neinast, M., Tapia, E.E., van de Weijer, T., Hoeks, J., Schrauwen-Hinderling, V.B., Blair, M.C., Bornstein, M.R., Hesselink, M.K.C., Schrauwen, P., et al., 2022. A randomized placebo-controlled clinical trial for pharmacological activation of BCAA catabolism in patients with type 2 diabetes. *Nat. Commun.* 13, 3508.
- Wada, E., Kobayashi, M., Kohno, D., Kikuchi, O., Suga, T., Matsui, S., Yokota-Hashimoto, H., Honzawa, N., Ikeuchi, Y., Tsuneoka, H., et al., 2021. Disordered branched chain amino acid catabolism in pancreatic islets is associated with postprandial hypersecretion of glucagon in diabetic mice. *J. Nutr. Biochem.* 97, 108811.
- Wang, T.J., Larson, M.G., Vasan, R.S., Cheng, S., Rhee, E.P., McCabe, E., Lewis, G.D., Fox, C.S., Jacques, P.F., Fernandez, C., et al., 2011. Metabolite profiles and the risk of developing diabetes. *Nat. Med.* 17, 448–453.
- Wei, S., Zhao, J., Wang, S., Huang, M., Wang, Y., Chen, Y., 2018. Intermittent administration of a leucine-deprived diet is able to intervene in type 2 diabetes in db/db mice. *Helix* 4, e00830.
- Wei, Z., Liu, X., Cheng, C., Yu, W., Yi, P., 2020. Metabolism of amino acids in cancer. *Front. Cell Dev. Biol.* 8, 603837.
- White, P.J., McGarrah, R.W., Grimsrud, P.A., Tso, S.C., Yang, W.H., Haldeman, J.M., Grenier-Larouche, T., An, J., Lapworth, A.L., Astapova, I., et al., 2018. The BCCKDH kinase and phosphatase integrate BCAA and lipid metabolism via regulation of ATP-citrate lyase. *Cell Metabol.* 27, 1281–1293.e7.
- Winther-Sørensen, M., Galsgaard, K.D., Santos, A., Trammell, S.A.J., Sulek, K., Kuhre, R. E., Pedersen, J., Andersen, D.B., Hassing, A.S., Dall, M., et al., 2020. Glucagon acutely regulates hepatic amino acid catabolism and the effect may be disturbed by steatosis. *Mol. Metabol.* 42, 101080.
- Würtz, P., Soininen, P., Kangas, A.J., Rönnemaa, T., Lehtimäki, T., Kähönen, M., Viikari, J.S., Raitakari, O.T., Ala-Korpela, M., 2013. Branched-chain and aromatic amino acids are predictors of insulin resistance in young adults. *Diabetes Care* 36, 648–655.
- Yamamoto, K., Tsuchisaka, A., Yukawa, H., 2017. Branched-chain amino acids. *Adv. Biochem. Eng. Biotechnol.* 159, 103–128.
- Yoneshiro, T., Wang, Q., Tajima, K., Matsushita, M., Maki, H., Igarashi, K., Dai, Z., White, P.J., McGarrah, R.W., Ilkayeva, O.R., et al., 2019. BCAA catabolism in brown fat controls energy homeostasis through SLC25A44. *Nature* 572, 614–619.
- Yu, J.Y., Cao, N., Rau, C.D., Lee, R.P., Yang, J., Flach, R.J.R., Petersen, L., Zhu, C., Pak, Y. L., Miller, R.A., et al., 2023. Cell-autonomous effect of cardiomyocyte branched-chain amino acid catabolism in heart failure in mice. *Acta Pharmacol. Sin.* 44, 1380–1390.
- Zeigerer, A., Sekar, R., Kleinert, M., Nason, S., Habegger, K.M., Müller, T.D., 2021. Glucagon's metabolic action in health and disease. *Compr. Physiol.* 11, 1759–1783.
- Zhang, S., Zeng, X., Ren, M., Mao, X., Qiao, S., 2017. Novel metabolic and physiological functions of branched chain amino acids: a review. *J. Anim. Sci. Biotechnol.* 8, 10.
- Zhao, S., Zhou, L., Wang, Q., Cao, J.H., Chen, Y., Wang, W., Zhu, B.D., Wei, Z.H., Li, R., Li, C.Y., et al., 2023. Elevated branched-chain amino acid promotes atherosclerosis progression by enhancing mitochondrial-to-nuclear H(2)O(2)-disulfide HMGB1 in macrophages. *Redox Biol.* 62, 102696.
- Zhou, M., Shao, J., Wu, C.Y., Shu, L., Dong, W., Liu, Y., Chen, M., Wynn, R.M., Wang, J., Wang, J., et al., 2019. Targeting BCAA catabolism to treat obesity-associated insulin resistance. *Diabetes* 68, 1730–1746.